

# Numerical Simulation of Viscoelastic Fluid Flow Past a Cylinder on a Streamfunction Coordinate System

I. HUSAIN AND O. P. CHANDNA

*Department of Mathematics and Statistics and Fluid Dynamics Research Institute,  
University of Windsor, Windsor, Ontario, Canada N9B 3P4*

Received December 13, 1991; revised September 29, 1992

---

Steady two-dimensional flow of a viscoelastic fluid past a streamlined cylinder is numerically modeled using the von Mises coordinates. The governing equations for a second-order fluid flow past the cylinder are first transformed into a streamfunction coordinate system  $(\phi, \psi)$ , where  $\psi$  is the streamfunction of the flow. Taking  $\phi = x$ , the von Mises coordinates  $(x, \psi)$  are obtained and the governing equations reduced to a system of two equations in two unknowns  $\gamma(x, \psi)$  and  $\omega(x, \psi)$  which are solved subject to the appropriate boundary conditions in the von Mises computational domain. Several approximation formulas for the vorticity on the surface of the cylinder are derived and employed in obtaining the solutions at various Reynolds and Weissenberg numbers for two specific cross sections. © 1993 Academic Press, Inc.

---

## 1. INTRODUCTION

The modelling of flow past submerged bodies constitutes an important class of problems which has and continues to receive much attention. Many methods exist to obtain the solution to such problems [1-3]. However, the need to improve the mathematical formulation as well as the method of solution is always present. In this paper, we present a method that is well suited for studying flow past a cylinder before separation of flow occurs. This method offers several computational advantages in its formulation of this problem, both for Newtonian and non-Newtonian flows.

The idea for this method originated from Martin's [4] theoretical study of steady viscous incompressible flows. He introduced a streamfunction coordinate system  $(\phi, \psi)$ , where the coordinate  $\psi$  is taken as the streamfunction of the flow while the coordinate  $\phi$  is at first left arbitrary. Since the fluid moves along the streamlines, the  $(\phi, \psi)$  coordinate system is a natural choice for the application of theoretical analysis or numerical computations. These coordinates reduce to von Mises [5] coordinates if the arbitrary family of curves  $\phi(x, y) = \text{constant}$  is chosen to be  $x = \text{constant}$ . Barron [6] made this choice in a study of plane potential

incompressible flow over symmetric airfoils. The von Mises transformation easily maps the flow region of flow past a cylinder into a rectangular domain in the computational plane  $(x, \psi)$  suitable for finite differencing.

The use of coordinate transformation is common in the study of a variety of non-Newtonian flows especially of flow past submerged bodies. Pilate and Crochet [1] employed orthogonal curvilinear coordinates in considering the plane flow of a viscoelastic fluid past circular and elliptical cylinders taking inertia effects into account while Dairenieh and McHugh [7] neglected inertia effects in studying the axisymmetric flow of second- and third-order fluids past a spheroidal body using several coordinate systems. More recently, Andre and Clermont [8] reconsidered the die swell problem, employing a change of variables using streamlines to transform an irregular physical domain into a rectangular one.

In this paper, we consider the steady plane flow of a second-order fluid past a cylinder of streamlined cross section. This problem is formulated in von Mises coordinates and the mathematical difficulties arising from the nonlinear governing equations necessitates the use of numerical methods to solve these equations. We also consider the combined effect of the nonlinear inertia terms and the nonlinear terms in the viscosity part of the constitutive equation for the second-order fluid in order to study how the viscous flow is affected by a slight elasticity of the fluid. Since second-order fluid flow remains valid as long as the corresponding Newtonian flow is only slightly perturbed, the solutions obtained make sense only if they do not differ considerably from the Newtonian solutions, which is actually the case. In the von Mises formulation, the vorticity on no-slip boundaries is not known a priori. Therefore, the vorticity values on these boundaries must be determined by some approximation formulas. We have derived a number of vorticity approximation formulas in von Mises coordinates.

The plan of this paper is as follows: in Section 2, the

equations governing steady, plane, incompressible flow of a second-order fluid are written in two suitable forms. The first form is when  $u, v$ , and  $p$  are the dependent variables in the physical plane  $(x, y)$ . The second form is when  $\omega(\phi, \psi)$ ,  $h(\phi, \psi)$ , and the three metric coefficients of the natural net  $(\phi, \psi)$  are the dependent variables. In Section 3, we employ von Mises coordinates by choosing  $\phi = x$  to obtain a system of two equations in two unknowns  $y(x, \psi)$  and  $\omega(x, \psi)$ . The appropriate boundary conditions for the flow past a cylinder of streamlined cross section are prescribed on the von Mises computational domain and various approximation formulas for the vorticity on the surface of the cylinder are also derived in this section. In Section 4, the numerical method of solution is presented. In the final section, a number of vorticity approximation formulas are employed in obtaining the numerical solutions at various Reynolds and Weissenberg numbers for two specific cross sections and the results obtained are discussed.

## 2. EQUATIONS OF MOTION

The steady plane incompressible flow of a second-order fluid in the absence of body forces is governed by

$$u_x + v_y = 0 \tag{1}$$

$$\begin{aligned} \rho(uu_x + vv_y) + p_x \\ = \mu \nabla^2 u + \alpha_1 [u(\nabla^2 u)_x + v(\nabla^2 u)_y \\ + u_x \nabla^2 u + v_x \nabla^2 v] + \frac{1}{4} (3\alpha_1 + 2\alpha_2) \{ |A_1|^2 \}_x \end{aligned} \tag{2}$$

$$\begin{aligned} \rho(uv_x + vv_y) + p_y \\ = \mu \nabla^2 v + \alpha_1 [u(\nabla^2 v)_x + v(\nabla^2 v)_y \\ + u_y \nabla^2 u + v_y \nabla^2 v] + \frac{1}{4} (3\alpha_1 + 2\alpha_2) \{ |A_1|^2 \}_y, \end{aligned} \tag{3}$$

where  $u$  and  $v$  are the horizontal and vertical components of velocity, respectively,  $p$  is the fluid pressure,  $\rho$  is the fluid density,  $\mu$  is the coefficient of viscosity,  $\alpha_1$  and  $\alpha_2$  are material constants,  $\nabla^2$  is the Laplacian operator, and  $|A_1|^2$  is given by

$$|A_1|^2 = 4(u_x)^2 + 4(v_y)^2 + 2(u_y + v_x)^2.$$

A second-order fluid may be considered as the limit of a simple fluid for small natural times. The first- and second-order equations of the well-known  $n$ th-order Rivlin-Ericksen equations of state are, respectively, the constitutive relations of a Newtonian and second-order fluid. When the flow is slow and slowly varying and the fluids under consideration are only slightly elastic, the second-order equation can be used with a certain degree of confidence. Dunn and Fosdick [9] found that if a second-order fluid is to be compatible with thermodynamics in the sense that all motions of

the fluid meet the Clausius-Duhem inequality and the assumption that the specific Helmholtz free energy of the fluid will be a minimum when the fluid is in equilibrium, then the material constants which characterize the fluid have to satisfy the following restrictions [9]:

$$\mu \geq 0, \quad \alpha_1 \geq 0, \quad \alpha_1 + \alpha_2 = 0.$$

Equations (1) to (3) form a system of three equations in three unknowns  $u(x, y)$ ,  $v(x, y)$ , and  $p(x, y)$ .

Defining an energy function  $h(x, y)$  and vorticity function  $\omega(x, y)$  by

$$\omega = v_x - u_y \tag{4}$$

$$\begin{aligned} h = p + \frac{1}{2} \rho(u^2 + v^2) - \alpha_1 (u \nabla^2 u + v \nabla^2 v) \\ - \frac{1}{4} (3\alpha_1 + 2\alpha_2) |A_1|^2 \end{aligned} \tag{5}$$

and non-dimensionalizing with respect to a characteristic length  $L$  and speed  $U_\infty$ , the flow equations in non-dimensional form are

$$u_x + v_y = 0 \tag{6}$$

$$\text{Re } h_x - \text{Re } v\omega + \omega_y + \text{We } v \nabla^2 \omega = 0 \tag{7}$$

$$\text{Re } h_y + \text{Re } u\omega - \omega_x - \text{We } u \nabla^2 \omega = 0 \tag{8}$$

$$v_x - u_y = \omega, \tag{9}$$

where  $\text{Re} = \rho U_\infty L / \mu$  is the Reynolds number and  $\text{We} = \alpha_1 U_\infty / \mu L$  is the Weissenberg number. The  $\text{We}$  number is the ratio of elastic effects to viscous effects. In view of the limitation on the second-order fluid model, the flow features obtained for such a fluid remains valid provided the  $\text{We}$  number is less than unity. Equations (6) to (9) form a system of four equations in four unknowns  $u(x, y)$ ,  $v(x, y)$ ,  $\omega(x, y)$ , and  $h(x, y)$ .

Equation (6) implies the existence of a streamfunction  $\psi(x, y)$  such that

$$\psi_x = -v, \quad \psi_y = u. \tag{10}$$

We take  $\phi(x, y) = \text{const}$  to be some arbitrary family of curves which generates with the streamlines  $\psi(x, y) = \text{const}$ , a curvilinear net  $(\phi, \psi)$  so that in the physical plane the independent variables  $x, y$  can be replaced by  $\phi, \psi$ . Let

$$x = x(\phi, \psi), \quad y = y(\phi, \psi) \tag{11}$$

define the curvilinear net with the squared element of arc length along any curve given by

$$ds^2 = E(\phi, \psi) d\phi^2 + 2F(\phi, \psi) d\phi d\psi + G(\phi, \psi) d\psi^2,$$

wherein

$$E = x_\phi^2 + y_\phi^2, \quad F = x_\phi x_\psi + y_\phi y_\psi, \quad G = x_\psi^2 + y_\psi^2.$$

Equation (11) can be solved to obtain  $\phi = \phi(x, y)$  and  $\psi = \psi(x, y)$  such that

$$x_\phi = J\psi_y, \quad x_\psi = -J\phi_y, \quad y_\phi = -J\psi_x, \quad y_\psi = J\phi_x$$

where

$$J = x_\phi y_\psi - x_\psi y_\phi = \pm \sqrt{EG - F^2}$$

is the transformation Jacobian and  $0 < |J| < \infty$ . Here we assume that the fluid flows along streamlines  $\psi = \text{const}$  in the direction of increasing  $\phi$  so that  $J > 0$  (cf. Martin [4]).

Kaloni and Siddiqui [10] transformed Eq. (7) to (9) into the  $(\phi, \psi)$  coordinates and obtained

$$\text{Re } h_\phi = \frac{F}{J} \omega_\phi - \frac{E}{J} \omega_\psi \quad (12)$$

$$\text{Re } h_\psi = \frac{G}{J} \omega_\phi - \frac{F}{J} \omega_\psi - \text{Re } \omega + \text{We } \nabla^2 \omega \quad (13)$$

$$\omega = \frac{1}{J} \left[ \left( \frac{F}{J} \right)_\phi - \left( \frac{E}{J} \right)_\psi \right] \quad (14)$$

$$\left( \frac{J}{E} \Gamma_{11}^2 \right)_\psi - \left( \frac{J}{E} \Gamma_{12}^2 \right)_\phi = 0, \quad (15)$$

where

$$\nabla^2 \omega = \frac{1}{J} \left[ \left( \frac{G\omega_\phi - F\omega_\psi}{J} \right)_\phi + \left( \frac{-F\omega_\phi + E\omega_\psi}{J} \right)_\psi \right].$$

Equations (12) to (15) are four partial differential equations in five unknowns  $E, F, G, h$ , and  $\omega$  as functions of  $\phi$  and  $\psi$ .

Having determined a solution of this system, the flow in the physical and the hodograph plane is described by (cf. Martin [4])

$$z = \int \frac{e^{ix}}{\sqrt{E}} [E d\phi + (F + iJ) d\psi],$$

$$\alpha = \int \frac{J}{E} [\Gamma_{11}^2 d\phi + \Gamma_{12}^2 d\psi]$$

$$u + iv = qe^{ix} = \frac{\sqrt{E}}{J} e^{ix}, \quad q = \sqrt{u^2 + v^2}.$$

The pressure in the physical plane is determined by Eq. (5).

The system of Eqs. (12) to (15) is under determined due to the arbitrariness of the curves  $\phi = \text{const}$ . This system can be made determinate in a number of ways by fixing these

curves. The appropriate choice of  $\phi$  depends on the problem under consideration. Barron [6], in a study of plane irrotational flow past bodies chose  $\phi = x$ , obtaining the von Mises coordinate system  $(x, \psi)$ . The formulation of the problem of flow past submerged bodies in the von Mises plane offers several computational advantages. Therefore, we transform and solve the equations governing the flow of a second-order fluid past a cylinder in the von Mises plane subject to the appropriate boundary conditions.

### 3. VON MISES FORMULATION

The flow past a cylinder in a second-order fluid is governed by the system of Eqs. (12) to (15). In the von Mises coordinates  $(x, \psi)$ , we have

$$E = 1 + y_x^2, \quad F = y_x y_\psi, \quad G = y_\psi^2, \quad J = y_\psi. \quad (16)$$

Employing (16) in Eqs. (12) to (15) with  $\phi = x$  and applying the integrability condition  $h_{x\psi} = h_{\psi x}$ , the governing equations in the von Mises plane are given by

$$\begin{aligned} y_\psi^2 y_{xx} + (1 + y_x^2) y_{\psi\psi} - 2y_x y_\psi y_{x\psi} &= y_\psi^3 \omega \quad (17) \\ y_\psi^4 \omega_{xx} + (1 + y_x^2) y_\psi^2 \omega_{\psi\psi} - 2y_x y_\psi^3 \omega_{x\psi} - y_\psi^4 \omega \omega_\psi \\ &- \text{Re } y_\psi^3 \omega_x + \text{We} [y_\psi^3 \omega_{xxx} - 2y_x y_\psi^2 \omega_{x\psi} \\ &+ (1 + y_x^2) y_\psi \omega_{\psi\psi} \\ &+ (2y_x y_\psi y_{x\psi} - 2y_\psi^2 y_{xx} - y_\psi^3 \omega) \omega_{x\psi} \\ &- y_\psi^3 \omega_x \omega_\psi + (2y_x y_\psi y_{xx} - 2(1 + y_x^2) y_{x\psi}) \omega_{\psi\psi}] = 0. \end{aligned} \quad (18)$$

Equation (15) is identically satisfied assuming  $y_{x\psi} = y_{\psi x}$ . The system of two nonlinear partial differential equations (17) and (18) in two unknowns  $y(x, \psi)$  and  $\omega(x, \psi)$  is solved numerically with the appropriate boundary conditions for  $y$  and  $\omega$ . Having obtained  $y(x, \psi)$ , the horizontal and vertical velocity components in the von Mises variables are given by

$$u = \psi_y = \frac{1}{y_\psi}, \quad v = -\psi_x = \frac{y_x}{y_\psi} = uy_x. \quad (19)$$

Since  $y_{x\psi} = y_{\psi x}$ , it follows that  $u(x, \psi)$  and  $v(x, \psi)$  also satisfy

$$u_x + uv_\psi - vu_\psi = 0. \quad (20)$$

### Boundary Conditions

We consider the steady uniform flow of a second-order fluid over an infinite cylinder of arbitrary streamlined cross section. We assume that any cross section of the cylinder

parallel to the  $(x, y)$  plane is symmetric with respect to the  $x$ -axis with the upper half given by  $y = f(x)$  and the flow at large distance from the cylinder is a uniform stream parallel to the positive  $x$ -direction as shown in Fig. 1. The flow is also assumed to be symmetric over the cylinder with respect to the  $x$ -direction and, therefore, we consider only the upper half of the physical plane. This flow region maps into the upper half of the von Mises plane. A rectangular computational domain is chosen in the  $(x, \psi)$  plane and the appropriate boundary conditions for  $y$  and  $\omega$  prescribed on all four sides as shown in Fig. 2. The boundary conditions for  $y$  and  $\omega$  are as follows:

*Boundary Conditions for  $y(x, \psi)$*

Left boundary (upstream),  $y = \psi$

Top boundary ( $\psi = \psi_{max}$ ),  $y = \psi$

Bottom boundary ( $x$ -axis),

$$y = \begin{cases} f(x), & x_L \leq x \leq x_T \\ 0, & x < x_L \text{ and } x > x_T \end{cases}$$

Right boundary (downstream),  $y_{\psi\psi} = y_{\psi}^3 \omega$

(assuming  $y_x \ll y_{\psi}$  along this boundary).

*Boundary Conditions for  $\omega(x, \psi)$*

Left boundary (upstream),  $\omega = 0$

Top boundary ( $\psi = \psi_{max}$ ),  $\omega = 0$

Right boundary (downstream),  $\omega_x = 0$

Bottom boundary ( $x$ -axis),

$$\omega = \begin{cases} -\frac{1}{2}(u^2 + v^2)_{\psi}, & x_L \leq x \leq x_T \\ 0, & x < x_L \text{ and } x > x_T. \end{cases}$$

The conditions at the exit (right boundary) comes from the observations that the vorticity far from the body is

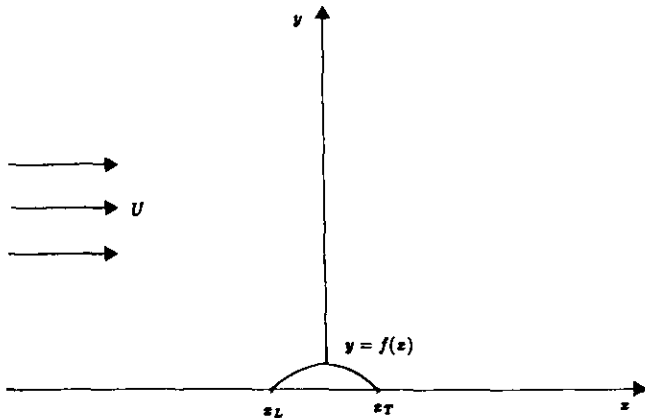


FIG. 1. Physical plane.

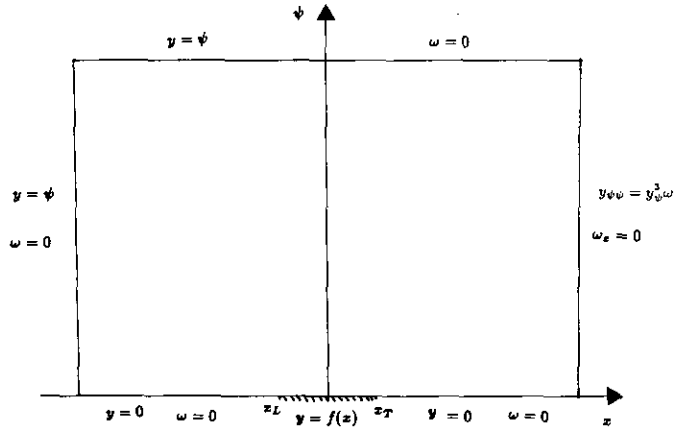


FIG. 2. Computational domain and boundary conditions.

concentrated in a thin streak downstream with maximum strength inversely proportional to the distance and the variation of the dependent variable  $y$  in the  $x$ -direction is much less than that in the  $\psi$ -direction along this boundary. Therefore, the appropriate exit condition for the vorticity is obtained by equating the values of  $\omega$  on the last two grid lines. Noting that  $y_x \ll y_{\psi}$ , (17) yields the boundary condition for  $y$  at the exit.

**Vorticity Approximation Formulas**

The approximation formula for the vorticity on the surface of the cylinder is derived as follows; employing Eq. (19) in Eq. (17), we obtain

$$\omega(x, \psi) = v_x - uu_{\psi} - 2vv_{\psi} - \frac{v}{u}u_x + \frac{v^2}{u}u_{\psi}.$$

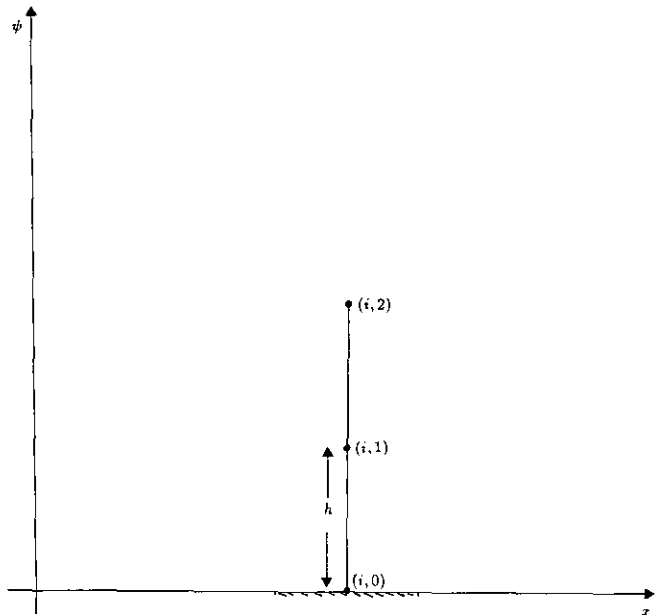


FIG. 3. Typical grid points on and near the cylinder.

Eliminating  $u_x$  using Eq. (20), the vorticity is given by

$$\omega(x, \psi) = v_x - \frac{1}{2} (q^2)_{\psi},$$

where  $q^2 = u^2 + v^2$  is the speed of the flow. Since  $v = 0$  for every  $x$  on the bottom boundary  $\psi = 0$ , the vorticity on the surface of the cylinder is given by

$$\omega(x, 0) = -\frac{1}{2} (q^2)_{\psi}. \quad (21)$$

To solve Eqs. (17) and (18) numerically, the rectangular domain in the  $(x, \psi)$  plane is covered by a uniform rectangular grid of width  $k$  in the  $x$ -direction and  $h$  in the  $\psi$ -direction. Various first- and second-order formulas of Eq. (21) can be obtained by considering Taylor's series expansion at internal grid points. A typical grid point  $(i, 0)$  on the surface of the cylinder and the adjacent internal points  $(i, 1)$  and  $(i, 2)$  are shown in Fig. 3.

Expanding  $q^2$  at the internal grid points about  $(i, 0)$ , we have

$$(q^2)_{i,1} = (q^2)_{i,0} + h[(q^2)_{\psi}]_{i,0} + \frac{h^2}{2} [(q^2)_{\psi\psi}]_{i,0} + \dots \quad (22)$$

$$(q^2)_{i,2} = (q^2)_{i,0} + 2h[(q^2)_{\psi}]_{i,0} + 2h^2[(q^2)_{\psi\psi}]_{i,0} + \dots \quad (23)$$

Employing (21) in (22) and solving for  $\omega_{i,0}$ , we obtain

$$\omega_{i,0} = -\frac{1}{2h} [(q^2)_{i,1} - (q^2)_{i,0}] + O(h). \quad (24)$$

The no-slip condition on the surface of the cylinder reduces Eq. (24) to

$$\omega_{i,0} = -\frac{1}{2h} (q^2)_{i,1} \quad (25)$$

which is a first-order approximation for the vorticity on the surface of the cylinder.

The derivation of (25) is similar to the derivation of boundary vorticity approximation formulas in the stream-function-vorticity formulation [11]. Subtracting (23) from  $4 \times (22)$  and solving for  $\omega_{i,0}$  yields a second-order formula for the vorticity on the surface of the cylinder given by

$$\omega_{i,0} = -\frac{1}{4h} [4(q^2)_{i,1} - (q^2)_{i,2}]. \quad (26)$$

Similarly, various other second-order and higher order approximation formulas can be obtained for the vorticity on

the surface of the cylinder. Two other formulas of second order are given by

$$\omega_{i,0} = -\frac{1}{12h} [9(q^2)_{i,1} - (q^2)_{i,3}] \quad (27)$$

$$\omega_{i,0} = -\frac{1}{24h} [16(q^2)_{i,1} - (q^2)_{i,4}]. \quad (28)$$

For convenience, we symbolically denote the boundary vorticity expression given by (25) the (1, 1) formula, where the first one indicates that it is a first-order approximation involving the values of the speed of the flow at the first grid points above the surface of the cylinder. Thus, Eq. (26) is the (2, 1, 2) formula, Eq. (27) is the (2, 1, 3) formula, and finally Eq. (28) is the (2, 1, 4) formula. We employed various boundary approximation formulas in obtaining the numerical solutions of our flow problem.

#### 4. METHOD OF SOLUTION

As stated, Eqs. (17) and (18) are solved numerically on a rectangular computational domain for  $y$  and  $\omega$ , respectively. This domain in the  $(x, \psi)$  plane is covered by a uniform mesh of width  $k$  in the  $x$ -direction and  $h$  in the  $\psi$ -direction. Second-order accurate central difference formulas are used to approximate all derivatives in (17) and (18). A numerical solution for a given cross section of the cylinder and value of  $Re$  and  $We$  is obtained by an overall iterative procedure subject to the stated boundary conditions. The iterative procedure used here is successive over-relaxation (SOR). At any iteration level, Eq. (17) is solved at every unknown gridpoint for  $y$ . Having obtained  $y$ , the vorticity on the surface of the cylinder is calculated using one of the formulas derived above. Equation (18) is then solved for  $\omega$  at every internal grid point. This procedure is repeated until  $y$  and  $\omega$  have converged to limits, within an acceptable tolerance, at every internal grid point and also at every boundary grid point at which they are not known. The solution procedure employed here is based on obtaining the Newtonian flow solution first [7]. This solution is then the starting point for the iterative procedure to obtain the solutions for all  $We > 0$ . The vorticity values on the surface of the cylinder are calculated directly using the various approximation formulas. To reduce round-off error, all computations are carried out in double precision. Finally, in the overall iterative procedure, the criterion for stopping iterations was a test on two consecutive values of  $y$  and  $\omega$ ; if the difference between two values was less than  $10^{-4}$ ; the computation was stopped.

## 5. NUMERICAL RESULTS

We considered the flow over a cylinder of infinite length for two different cross sections given by

$$y = f_1(x) = 0.2 \sqrt{0.25 - x^2}$$

$$y = f_2(x) = 0.1(1 - 2x) \sqrt{1 - 4x^2}.$$

For streamlined bodies such as the cylinders considered here, separation of flow, if it occurs, does so near the rear of the body and the consequent wake is narrow. Since for a second-order fluid, separation of flow occurs at approximately the same Reynolds number as for a Newtonian fluid [1], we have restricted our flow to very low Reynolds numbers, before the development of a reverse flow region behind the cylinders, so that the von Mises formulation can be applied accurately to analyze the flow. At  $Re = 40$ , the results obtained suggest possibly that the effects of

separation have become prominent and therefore higher Reynolds numbers were not attempted.

After some investigation with the boundaries, the final computational domain was chosen to extend from  $-5$  to  $10$  in the  $x$ -direction and from  $0$  to  $4$  in the  $\psi$ -direction. On this domain, three grids of different densities were used,  $151 \times 41$ ,  $167 \times 61$ , and  $177 \times 71$ . After checking the independence of the solutions obtained to changes in the grid sizes, it was found that the medium grid containing  $167 \times 61$  points offered sufficient resolution for the Reynolds numbers considered here and was used to calculate all the flow quantities.

For Newtonian flow, the distribution of vorticity over the surface of both cylinders obtained using the  $(2, 1, 2)$  formula are shown in Figs. 4 and 5. The vorticity over the surface of both cylinders obtained from the other approximation formulas showed similar distributions as in Fig. 4 and 5, decreasing monotonically with increasing Reynolds number. It is, therefore, sufficient to give the minimum

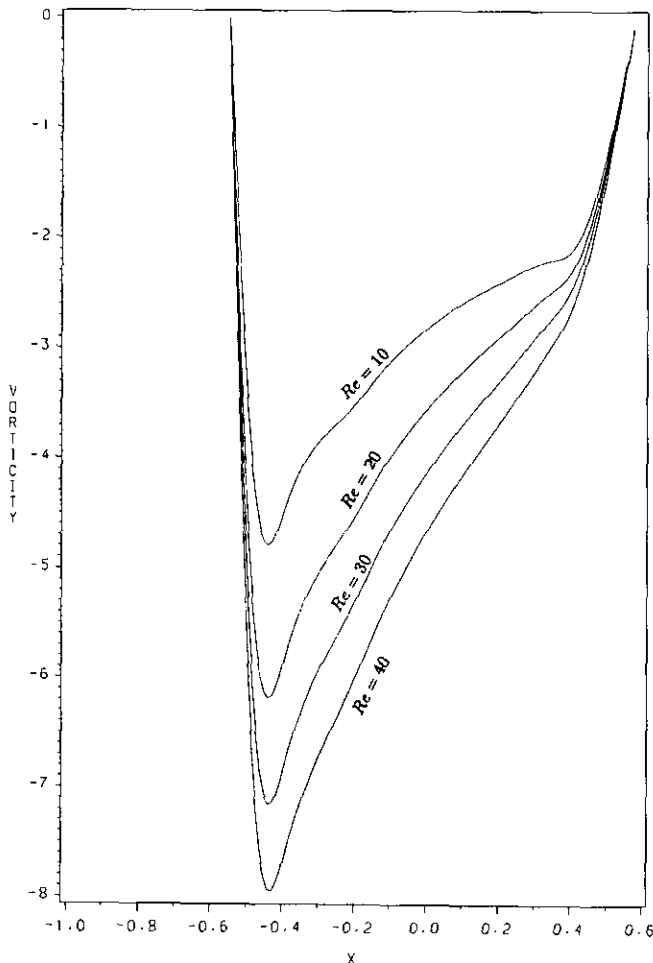


FIG. 4. The vorticity distribution over the surface of the cylinder  $y = f_1(x)$  for  $We = 0$ .

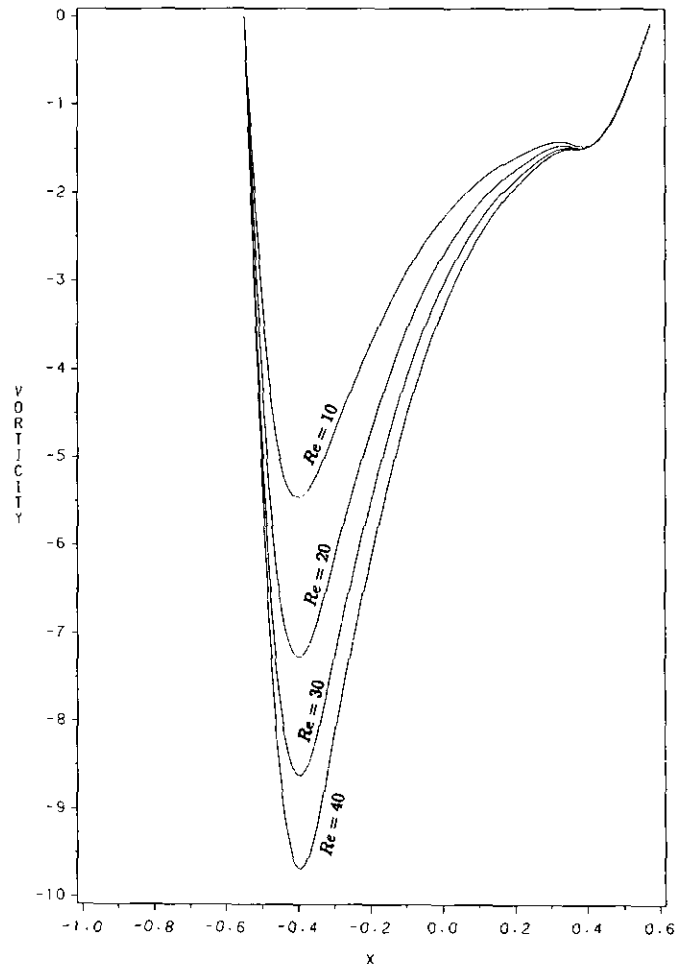


FIG. 5. Distribution of vorticity over the cylinder surface  $y = f_2(x)$  for  $We = 0$ .

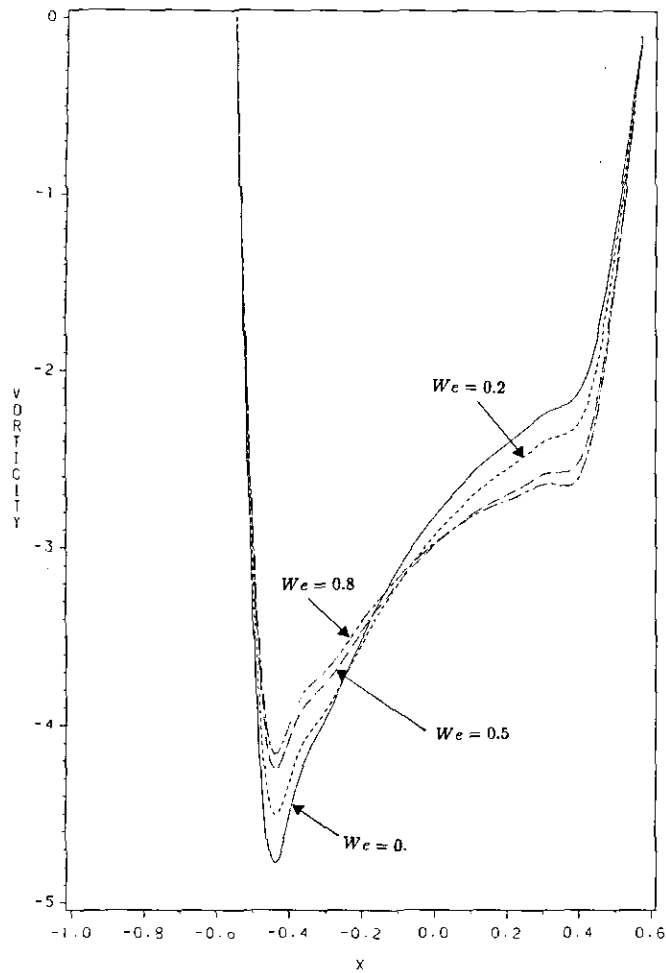


FIG. 6. The vorticity distribution over the surface of the cylinder  $y = f_1(x)$  at  $Re = 10$ .

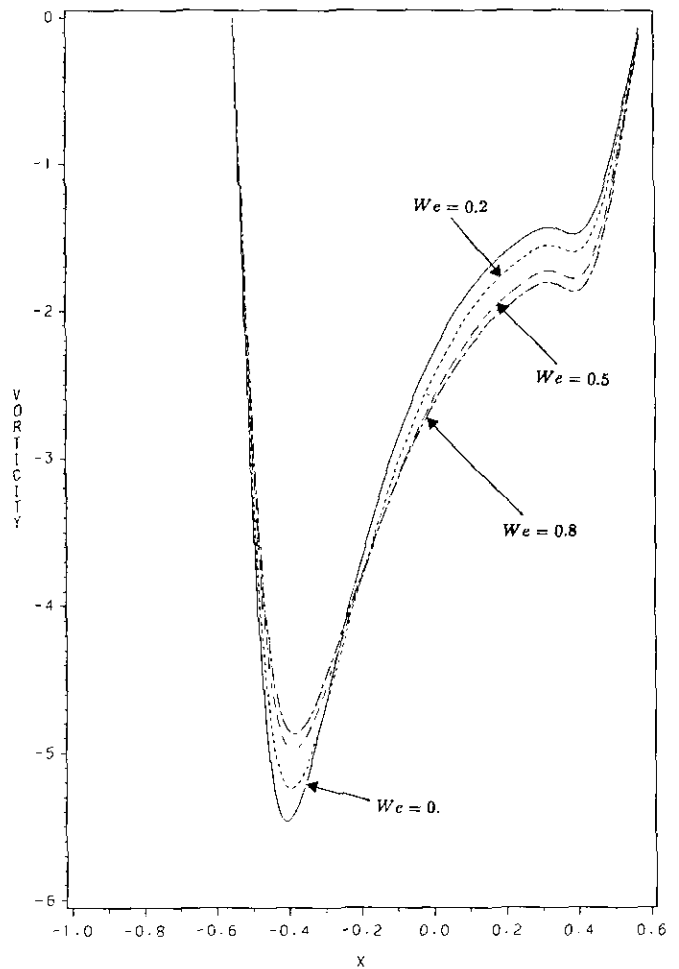


Fig. 7. Distribution of vorticity over the cylinder surface  $y = f_2(x)$  at  $Re = 10$ .

TABLE I

Minimum Vorticity as a Function of Re and Approximation Formula

Reynolds number	Vorticity approximation formula	Minimum Vorticity	
		$y = f_1(x)$	$y = f_2(x)$
10	(2, 1, 2)	-4.461	-5.452
	(2, 1, 3)	-4.331	-5.237
	(2, 1, 4)	-4.249	-5.115
20	(2, 1, 2)	-5.816	-7.263
	(2, 1, 3)	-5.612	-6.934
	(2, 1, 4)	-5.480	-6.743
30	(2, 1, 2)	-6.801	-8.619
	(2, 1, 3)	-6.524	-8.183
	(2, 1, 4)	-6.343	-7.926
40	(2, 1, 2)	-7.620	-9.686
	(2, 1, 3)	-7.266	-9.147
	(2, 1, 4)	-7.035	-8.830

TABLE II

Minimum Vorticity as a Function of Re and We Numbers

Reynolds number	Weissenberg number	Minimum Vorticity	
		$y = f_1(x)$	$y = f_2(x)$
10	0.2	-4.27	-5.24
	0.5	-4.04	-4.98
	0.8	-3.96	-4.86
20	0.2	-5.39	-6.73
	0.5	-4.98	-6.21
	0.8	-4.77	-5.93
30	0.2	-6.19	-7.81
	0.5	-5.64	-7.08
	0.8	-5.35	-6.60
40	0.2	-6.79	-8.64
	0.5	-6.15	-7.77
	0.8	-5.80	-7.17

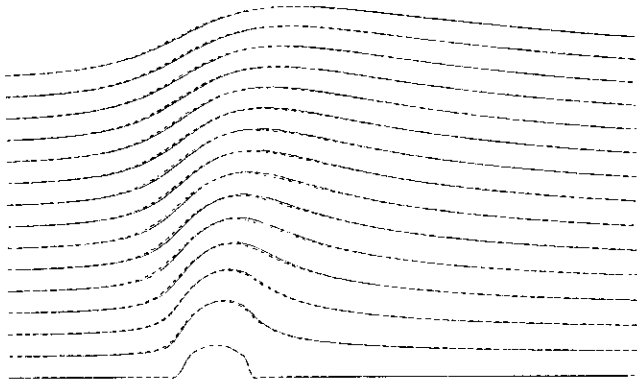


FIG. 8. Streamlines for the cylinder  $y = f_1(x)$  at  $Re = 10$ ,  $We = 0.2$ .

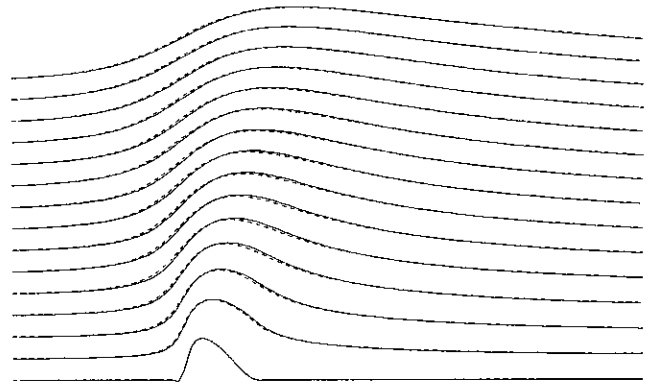


FIG. 11. Streamlines for the cylinder  $y = f_2(x)$  at  $Re = 10$ ,  $We = 0.2$ .

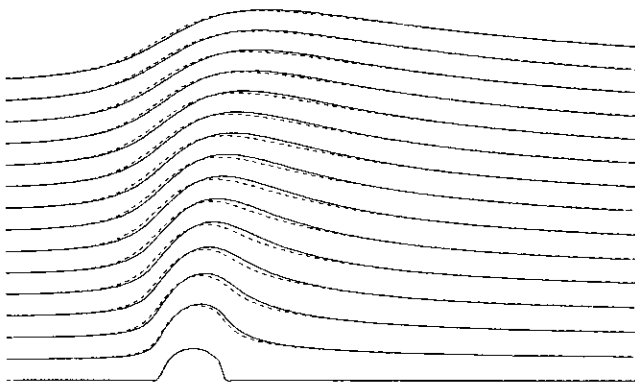


FIG. 9. Streamlines for the cylinder  $y = f_1(x)$  at  $Re = 10$ ,  $We = 0.5$ .

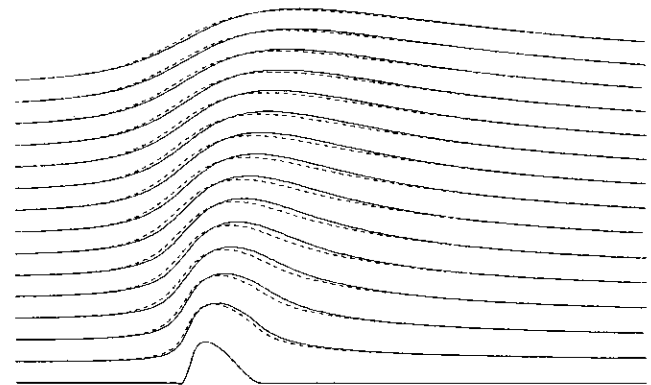


FIG. 12. Streamlines for the cylinder  $y = f_2(x)$  at  $Re = 10$ ,  $We = 0.5$ .

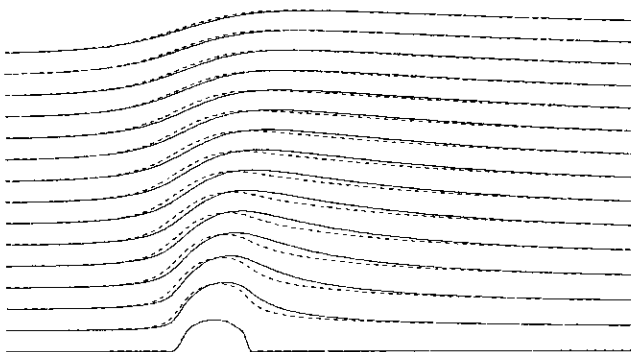


FIG. 10. Streamlines for the cylinder  $y = f_1(x)$  at  $Re = 30$ ,  $We = 0.8$ .

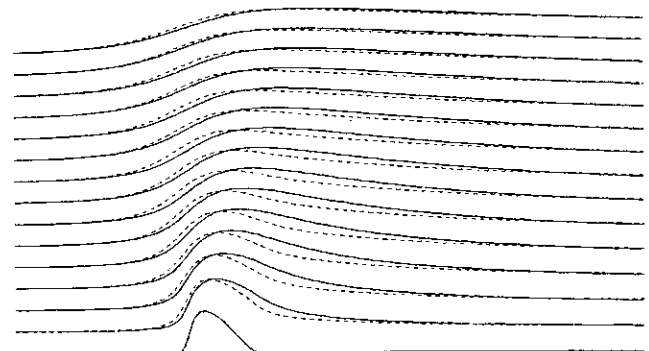


FIG. 13. Streamlines for the cylinder  $y = f_1(x)$  at  $Re = 30$ ,  $We = 0.8$ .



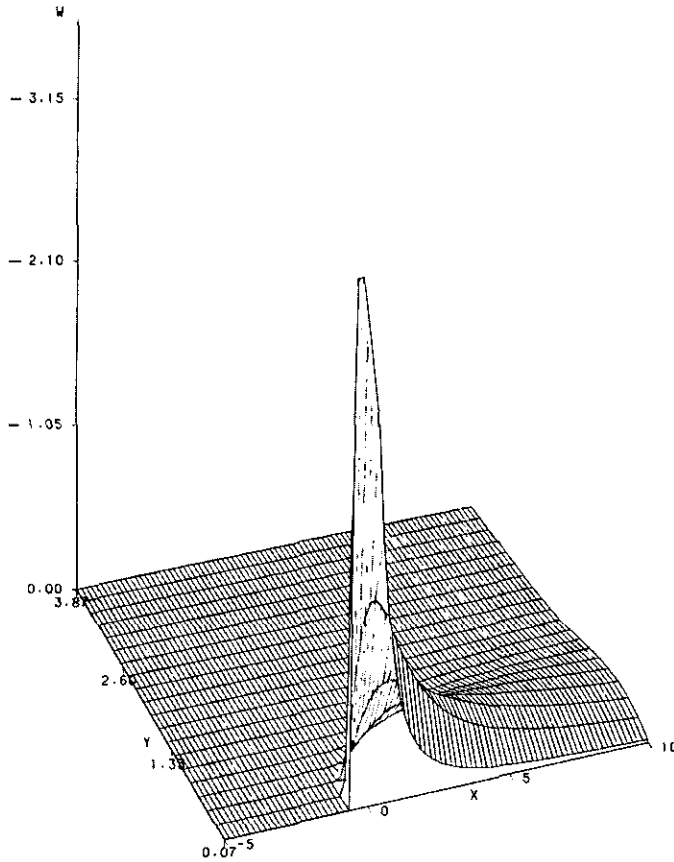


FIG. 14. Distribution of vorticity in the physical plane (excluding the cylinder  $y = f_1(x)$ ) at  $Re = 30$ ,  $We = 0$ .

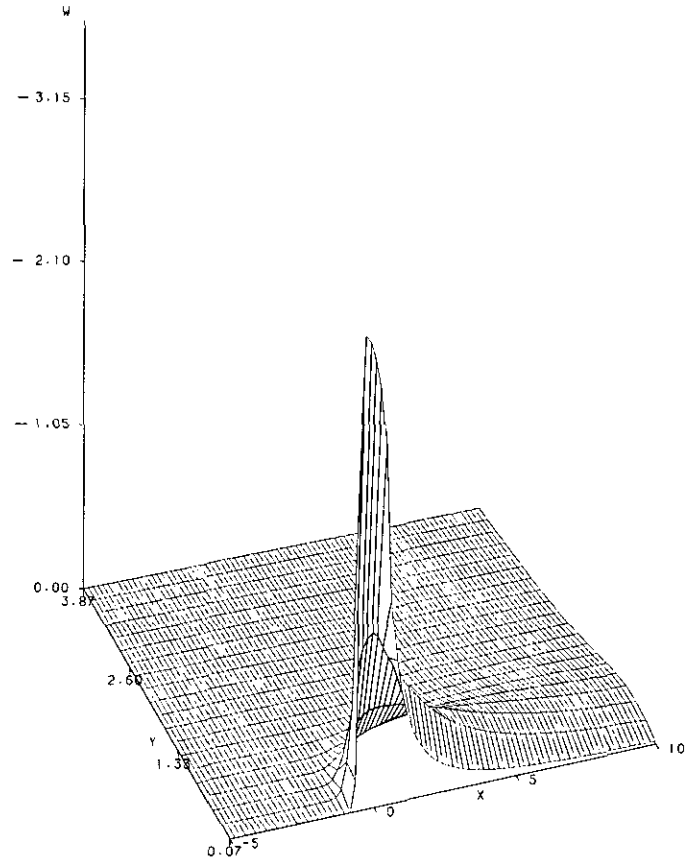


FIG. 15. Distribution of vorticity in the physical plane (excluding the cylinder  $y = f_1(x)$ ) at  $Re = 30$ ,  $We = 0.5$ .

vorticity values on the surface of both cylinders as a function of the Reynolds number for the second-order formulas as shown in Table I. The values are in reasonable agreement for both cylinders at lower Reynolds numbers while showing a significant difference at  $Re = 40$ , indicating possibly the onset of separation. Only second-order formulas were employed to approximate the surface vorticity since the value of the speed at every internal grid point is also second-order accurate.

Figures 6 and 7 show the distribution of surface vorticity for both cylinders at various  $We$  numbers for a fixed Reynolds number. In both cases, as the elasticity of the fluid increases, the surface vorticity increases. A similar trend is observed at all Reynolds numbers considered here as shown in Table II. All of the vorticity values have been obtained using the (2, 1, 2) formula. It is also found that the higher the  $We$  number, the higher the number of iterations required to achieve convergence. An upper limit is reached at about  $We = 0.85$  beyond which the numerical scheme becomes divergent.

Having obtained  $y(x_i, \psi_j)$  at every grid point  $(i, j)$  in the computational domain, the streamlines are easy to plot. To obtain the streamline  $\psi = \psi_j$ , the values of  $y$  are plotted for all values of  $i$  and a fixed value of  $j$ . Therefore, by varying  $j$ , some or all of the streamlines can be obtained. The streamline profile for the cylinder  $y = f_1(x)$  at  $Re = 10$  and  $30$  and various  $We$  numbers are shown in Fig. 8, 9, and 10. No appreciable difference is observed between the streamlines for Newtonian flow (solid lines) and that for low  $We$  numbers in Figs. 8 and 9. The effect of the slight elasticity of the fluid upon the velocity field is quite noticeable at higher  $Re$  and  $We$  numbers as can be seen in Fig. 10. The streamline patterns for the cylinder  $y = f_2(x)$  for various  $Re$  and  $We$  numbers are shown in Figs. 11, 12, and 13. The same effect of elasticity on the velocity field is observed here.

The distributions of vorticity in the physical plane are shown in Fig. 14, 15, 16, and 17 for both cylinders. These figures exclude the cylinders and show the vorticity distribution elsewhere in the computed flow domain. We observed

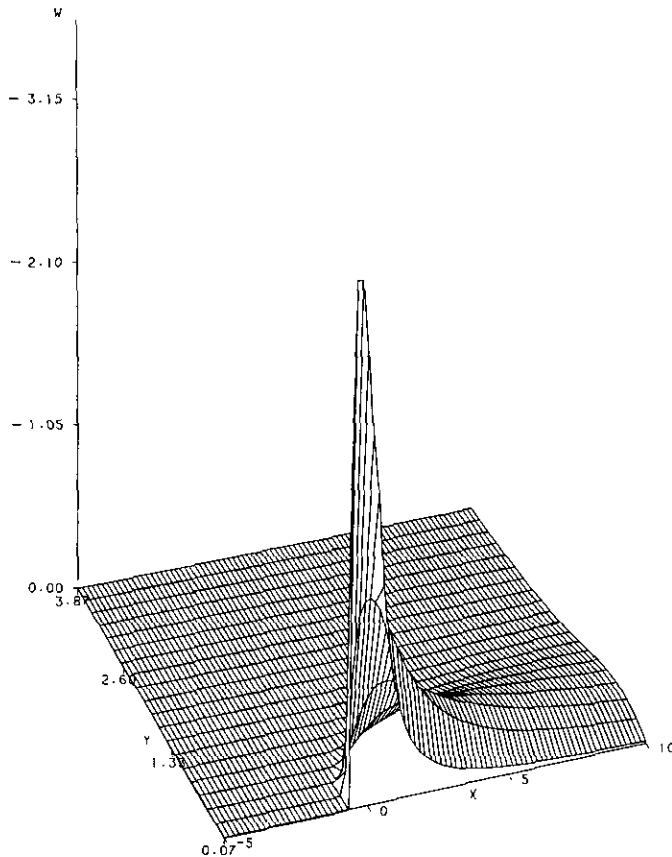


FIG. 16. The vorticity distribution in the physical plane (excluding the cylinder  $y = f_2(x)$ ) at  $Re = 30$ ,  $We = 0$ .

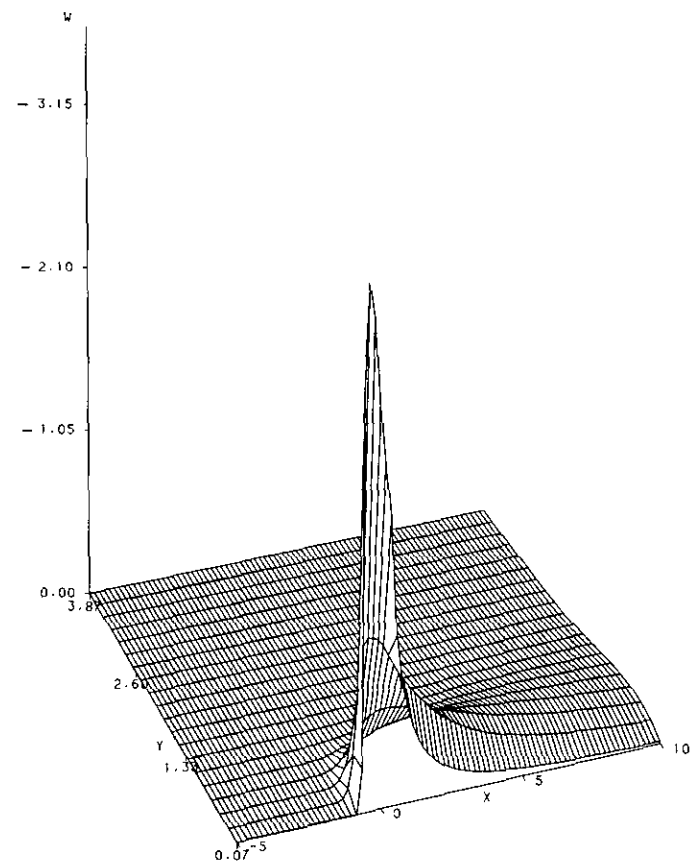


FIG. 17. The vorticity distribution in the physical plane (excluding the cylinder  $y = f_2(x)$ ) at  $Re = 30$ ,  $We = 0.5$ .

that non-zero vorticity is confined to the area adjacent to the cylinders and in the downstream region as expected. As the elasticity of the fluid increases, the vorticity increases throughout the flow domain for both cylinders.

## 6. CONCLUSIONS

Steady viscoelastic fluid flow past streamlined cylinders have been formulated in von Mises coordinates  $(x, \psi)$ . The governing equations consist of two equations in two unknowns  $\gamma(x, \psi)$  and  $\omega(x, \psi)$  which are solved subject to the appropriate boundary conditions in the von Mises computational domain. Various approximation formulas for the vorticity on the surface of the cylinders have been derived and employed in obtaining the solution. The von Mises coordinates easily maps the physical plane into a rectangular domain suitable for finite differencing. The main limitation of this formulation is that it cannot treat flows after separation occurs and reverse flow regions develop in the flow plane.

## ACKNOWLEDGMENT

The authors are grateful to the referees for their helpful comments and suggestions.

## REFERENCES

1. G. Pilate and M. J. Crochet, *J. Non-Newtonian Fluid Mech.* **2**, 323 (1977).
2. B. Fornberg, *J. Fluid Mech.* **98**, 819 (1980).
3. S. C. R. Dennis and G. Z. Zhang, *J. Fluid Mech.* **42**, 471 (1970).
4. M. H. Martin, *Arch. Rat. Mech. Anal.* **41**, 266 (1971).
5. R. von Mises, *Z. Angew. Math. Mech.* **7**, 425 (1927).
6. R. M. Barron, *Math. Comput. Simul.* **31**, 177 (1989).
7. I. S. Dairienich and A. J. McHugh, *J. Non-Newtonian Fluid Mech.* **19**, 81 (1985).
8. P. Andre and J. Clermont, *J. Non-Newtonian Fluid Mech.* **23**, 335 (1987).
9. J. Dunn and R. Fosdick, *Arch. Rat. Mech. Anal.* **56**, 191 (1974).
10. P. N. Kaloni and A. M. Siddiqui, *Int. J. Eng. Sci.* **21**, 1157 (1983).
11. D. A. Anderson, J. C. Tannehill, and R. H. Fletcher, *Computational Fluid Mechanics and Heat Transfer* (Hemisphere, New York, 1984).